Journal of Marine Research, 57, 165–187, 1999

Temporal variations of mixed-layer oceanic CO_2 at JGOFS-KERFIX time-series station: Physical versus biogeochemical processes

by Ferial Louanchi[1,2], Diana P. Ruiz-Pino[1] and Alain Poisson[1]

ABSTRACT

The seasonal and interannual variations in mixed-layer carbon dioxide in the Southern Ocean are analyzed from January 1990 to March 1995 at KERFIX time-series station (50°40S–69°25E). The temperature, salinity and chlorophyll time series are used as constraints on a simple box model to extrapolate total dissolved inorganic carbon (DIC), total alkalinity (TA) and oceanic CO_2 fugacity (fCO_2) over the five years of the monitoring. Results of the simulation are compared to all available observations.

Both measured and simulated DIC and TA give seasonal signals of 25 μmol/kg and 8 μeq/kg, respectively. In spite of a weak primary production about 70 gC/m^2/yr, the biological pump appears to play a significant role on seasonal and interannual variations in air-sea CO_2 exchanges. Its contribution varies from 10 to 45% of the total sea surface fCO_2 variations depending on the period. This area has been a sink for atmospheric CO_2 with annual mean values of -0.8 to -3.0 mol/m^2/yr during the whole period investigated. Annually the CO_2 sink is due to the balance between biological activity and mixing processes on fCO_2 inducing thermodynamically mediated variations. The sink's interannual variations appear to be mainly due to the high variability of the wind speeds and hence, of the mixed-layer depth.

The impact of the anthropogenic atmospheric CO_2 increase on oceanic fCO_2 is also investigated. The rate of increase of oceanic fCO_2 (0.6 μatm/yr) was half that of atmospheric fCO_2 (1.2 μatm/yr). The increase of the air-sea CO_2 gradient lead to an increase of the CO_2 sink of about 0.07 mol/m^2/yr (0.02 GtC/yr) over the five years investigated.

1. Introduction

Since the end of the eighteenth century, burned fossil fuel derived from industrial activity has resulted in an increase in atmospheric carbon dioxide (Keeling *et al.,* 1989). This increase may have an impact on the climate through the greenhouse effect and may ultimately result in a global temperature change. It appears from atmospheric CO_2 measurements that about half of the total fossil fuel emissions has remained in the atmosphere; the other half has been absorbed by terrestrial and oceanic compartments

1. Laboratoire de Physique et Chimie Marines, CNRS-Universite Pierre et Marie Curie, Case 134, 4 Place Jussieu, 75252 Paris Cedex 05, France.

2. Present address: Pennsylvania State University, Department of Meteorology, University Park, Pennsylvania, 16802, U.S.A. ***email: ferial@essc.psu.edu***

(Siegenthaler and Sarmiento, 1993). The amount of CO_2 absorbed by terrestrial and oceanic compartments as derived from direct or indirect estimates still exhibit large uncertainties (Houghton *et al.,* 1996). As long as the spatio-temporal variation of CO_2 exchanges among the three reservoirs is not known, long-term climate prediction will remain uncertain.

There are some good reasons to believe that the Antarctic Ocean (located south of the polar front) may have an important role in the air-sea CO_2 exchanges. On the one hand, it represents 12% of the global oceanic area. On the other hand, it is characterized by high wind speeds which favor gas exchange at the air-sea interface. A recent study has suggested that the future global carbon budget is mainly controlled by changes in Southern Ocean circulation (Sarmiento and Le Quéré, 1996).

The Southern Ocean is the least documented ocean. The scarcity of CO_2 data may be the cause of the wide range of estimates of the net air-sea CO_2 flux in the southern hemisphere. Atmospheric inverse models predict the Southern Ocean to be a source (see for example Tans *et al.,* 1990), whereas the oceanic data or models predict the Southern Ocean to be a sink (Sarmiento *et al.,* 1992). At the same time, *in situ* observations exhibit large spatial/temporal variabilities (Takahashi *et al.,* 1993; Poisson *et al.,* 1993). Indeed, even if most of the measurements carried out during the summer period demonstrate that this area is a net sink of CO_2 (Murphy *et al.,* 1991; Metzl *et al.,* 1995; Robertson and Watson, 1995), some source areas, such as the Kerguelen Plateau in the Indian sector, may exist (Poisson *et al.,* 1994). Only a few measurements are available for the winter period. Nonetheless, measurements in the Weddel gyre reveal some CO_2 sinks during the winter period (Hoppema *et al.,* 1995; Stoll *et al.,* 1998). Unfortunately, seasonal and shorter term variability is not very well documented for this remote area. The recent climatology of Takahashi *et al.* (1997) based on air-sea pCO_2 measurements suggests that this area is undersaturated all year round with an average of about -8 μatm.

To clearly understand the discrepancies in the various models mentioned above and to characterize the time/space resolution of the variability in the Southern Ocean, a first step could be a study of the process using the time series of atmospheric, biogeochemical and physical data. Due to the Southern Ocean distance and harshness, only a few programs have provided vital background information with respect to seasonal and interannual variability.

Now, however, a set of field measurements, including carbon parameters, has been obtained in the Southern Ocean by a five-year time series monitoring program (French JGOFS Program) called KERFIX (KERguelen island FIXe station). The KERFIX time series program, representing the open Antarctic Ocean, the so-called POOZ (Permanently Open Ocean Zone, Tréguer and Jacques, 1992) provided biogeochemical and physical data sets (Jeandel *et al.,* 1999), which may be used to evaluate the carbon budget and its temporal variability. The KERFIX site is located at 50°40S and 69°25E, southwest of Kerguelen Island and south of the Polar front (Fig. 1).

The aim of this study is to analyze the variation of air-sea CO_2 exchange at seasonal and

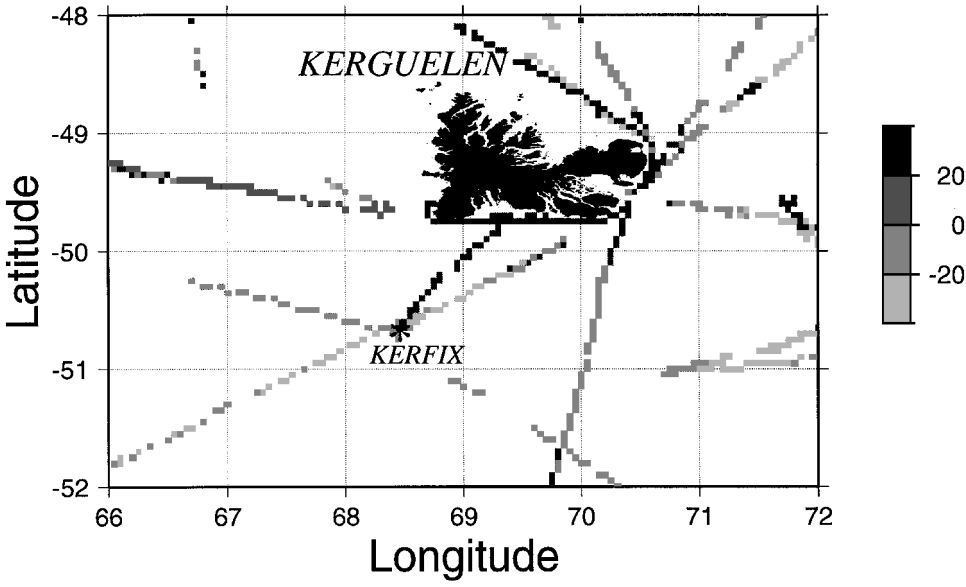

Figure 1. Location of the KERFIX time-series station. The air-sea CO_2 gradient (ΔfCO_2) is expressed in µatm and shows strong variability. These data are extracted from MINERVE (Mesures a l'INterface Eau-aiR de la Variabilité des Echanges de CO_2) cruises, which occurred in austral summer or fall periods in 1991 or 1993 (Louanchi, 1995).

interannual time scales by using KERFIX measurements and modeling techniques. The temporal variations of physical and biogeochemical processes were studied with regard to their impacts on the oceanic surface carbon cycle.

The KERFIX data (physical and biological) for the mixed layer will be presented in the first section. These data are used to constrain a model to extrapolate KERFIX information to seasonal and interannual time scales. The simple one-dimensional biogeochemical model is briefly described in the second section. The model results in terms of CO_2 seasonal and interannual variations are discussed in the third section. The impact of the natural processes involved in the oceanic carbon cycle on the air-sea CO_2 exchanges at seasonal and interannual time scale are quantified in the fourth and fifth sections, respectively. Finally, the impact of the anthropogenic atmospheric CO_2 increase on the air-sea CO_2 exchange is investigated for the KERFIX area.

2. KERFIX data

During the five years at KERFIX, monthly profiles of temperature, salinity, chlorophyll concentrations, total dissolved inorganic carbon (DIC), total alkalinity (TA) and nutrients were acquired (see Jeandel *et al.,* 1999 for a complete description of the program). This study will focus on the hydrological parameters (temperature and salinity), DIC, TA, nitrate and chlorophyll and their variability in time at the site.

The area around KERFIX presents much dynamic variability due to the Kerguelen Plateau in the eastern part and the polar front in the northern part. This variability is here illustrated by the air-sea CO_2 fugacity gradient (ΔfCO_2) distribution obtained by a synthesis of available data from this area (Fig. 1). Indeed, CO_2 undersaturations as well as neutral and CO_2 supersaturations were observed. As determined from MINERVE cruises (Poisson *et al.,* 1994), the KERFIX site and surrounding region was a CO_2 sink for most of the austral summer and fall (Fig. 1), and an increase of about 10 μatm was observed from February to April (Louanchi, 1995). The Kerguelen Plateau area exhibits the largest spatial variability reaching 50 μatm and the meridional fCO_2 variability across the Polar front is also quite large (Poisson *et al.,* 1993). The KERFIX site location was chosen according to practical constraints but also to avoid the Kerguelen island and polar front effects.

Figure 2 shows hydrological (T, S) and biological (Chl) mean values obtained in the mixed layed at KERFIX from January 1990 until March 1995. Satellite-derived wind speeds (Boutin and Etcheto, 1996) extracted for the nearest KERFIX location (50S–70E) and mixed-layer depth are also shown. Most of these parameters show a clear and marked seasonal cycle, except the wind speeds and the salinities which are more variable at interannual time scale.

Satellite-derived wind speeds show high levels all year round (Fig. 2a). The December–May level is about 8–11 m/s and the June–November level is about 12–14 m/s. The winds are particularly intense in late winter and spring between September and November. The averaged wind speed over the five years is 11.4 m/s. These high wind speeds increase the exchange of gases at the air-sea interface, as demonstrated previously by Liss and Merlivat (1986).

The monthly mixed-layer depths (MLD) (Fig. 2b) are deduced using the maximum density gradient criterion (based on observed profiles of discrete temperature and salinity measurements, see Park *et al.,* 1999). A summer (December–February) deep mixed-layer regime with values of about 60 m is encountered in this area, except for February 92 when the mixed-layer depth reaches 30 m. In winter period (June–September), the depth of the mixed-layer goes down to 200–240 m. A great interannual variability can be observed, particularly during the winter season. The temperature distribution (Fig. 2c) shows maximal values of about 4°C in February and March. Then the temperature decreases through August following the MLD increase (Fig. 2b). The seasonal temperature amplitude is always lower than 3°C in this area. The mean mixed-layer salinity (Fig. 2d) shows seasonal variations that are always lower than 0.15. A decreasing trend of the temperature starting in 1992 is observed, associated with an increasing trend of both MLD and salinity. These latter trends are consistent with the Antarctic Circumpolar Wave (ACW) propagation in the Southern Ocean (White and Peterson, 1996) and ACW appears to mainly drive interannual variability of hydrographic parameters around the KERFIX area (Ruiz-Pino *et al.,* in prep). Chlorophyll concentrations (Fig. 2e) reveal the occurrence of blooms during the period of stratification of the mixed layer. Indeed, Chl appears to vary from minimal values during the winter to reach 1.4 mg/m^3 during the summer period following the

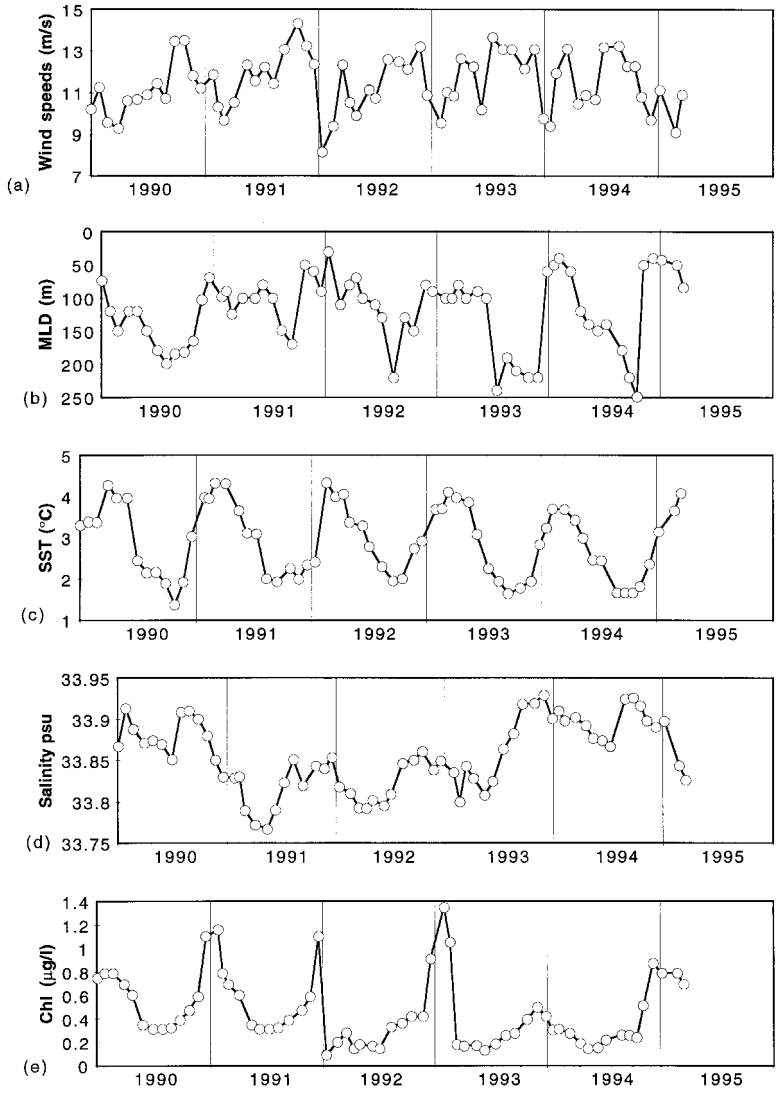

Figure 2. Distribution of monthly (a) wind speeds derived from satellite (Boutin and Etcheto, 1996), (b) Mixed-layer depth (calculated from the density profile for each period measurement) (c) temperature, (d) salinity, and (e) chlorophyll concentrations are the mean observations in the mixed-layer depth at KERFIX from 1990 to 1995.

stratification of the mixed layer. These values seem to be higher by 1 mg/m^3 than previous data reported by Jacques and Minas (1981) or Tréguer and Jacques (1992) for the POOZ area which is classified as a High-Nutrient/Low-Chlorophyll (HNLC) system (Minas and Minas, 1992). Cruises in mid to late summer (February to April) missed the maximal bloom. The chlorophyll concentration also presents a strong interannual variability. While

a low level of Chl biomass was measured in January 1992, an intense bloom was reported in December 1992 through February 1993. In contrast, a low level of chlorophyll is observed during the spring period in 1993 probably due to the deep mixed layer (Fig. 2b).

Located at the well-known roaring fifties, the high wind speed encountered at KERFIX would, therefore, lead to high levels of CO_2 exchanges at the air-sea interface. Because wind speeds are higher in September-October, a higher level of surface CO_2 during late winter rather than during summer might be expected. Moreover, the mixed layer exchanges CO_2 with the atmosphere but also with subsurface layers. In the ocean, the subsurface layers are enhanced in CO_2 by biological oxidation and solubility pump processes. On the contrary, in the surface oceanic layers, photosynthetic organisms reduce the CO_2 concentrations. This CO_2 surface-subsurface gradient induces an enhancement in surface CO_2 due to entrainment when the depth of the mixed layer increases during winter time. The Chl seasonal variation suggests that the CO_2 level in the mixed layer will be lower in summer than in winter. All these processes predetermine an increase of mixed-layer total CO_2 content (DIC) from summer through late winter. However, in terms of fCO_2 seasonal changes, one has to take into account the influence of SST variations which act as a counter-balance on a seasonal basis. Indeed, an increase of the temperature leads to an increase of the fCO_2 following the thermodynamical equilibrium of the DIC species (dissolved CO_2, carbonate and bicarbonate). A maximum fCO_2 level is then supposed to occur in summer period and a minimum around September. Moreover, an increase of temperature reduces the CO_2 solubility in the ocean leading to a CO_2 out-gasing under equilibrium conditions.

Less TA and DIC measurements were obtained during the five years than those obtained for hydrographical and biological properties. To analyze the air-sea CO_2 exchange at KERFIX station, it is necessary to get CO_2 information at the same time scale as the hydrographical parameters. Thus, to extrapolate the CO_2 parameters into the mixed layer, a simple biogeochemical model is used. Before the description of the one-dimensional (1D) model, the method of measurements of DIC and TA is briefly outlined below.

3. Modeling the CO_2 temporal distribution in the ocean mixed layer

a. Measurements of TA and DIC

Measurements of TA and DIC are adapted from the potentiometric method described by Edmond (1970). Samples of seawater are titrated with strong acid (HCl 0.1N) by using a burette Radiometer ABU 80 and a pHmeter Radiometer PHM80. The TA and DIC are calculated following the method of "US Department of Energy" (DOE, 1991). The acid is calibrated by using the samples prepared by Dr. Andrew Dickson (Scripps, La Jolla, California). For DIC and TA measurements, the potentiometric method gave accuracies of about 5 μeq/kg (0.3%) and 4 μmol/kg (0.2%), respectively (Poisson *et al.,* 1990) during the first period of KERFIX survey (1990–1992). Some calibration problems appeared for DIC results and the data obtained between 1990 and 1992 had to be discarded. During the year

1993, the accuracies of the measurements reach 1.4 μeq/kg for TA (0.06%) and 3.2 μmol/kg for DIC (0.14%).

b. Brief description of the model

A model is used to extrapolate the CO_2 variations over the five years of KERFIX monitoring. The model allows us to parameterize the main processes controlling the CO_2 in the oceanic mixed layer. These processes are the air-sea exchange, the carbonate chemistry, the phytoplankton uptake and release, and the exchange between surface and subsurface layers. In the model, each process contribution is calculated using the variation in wind-speed (W), mixed-layer depth (MLD), temperature (SST), salinity (S) and chlorophyll (Chl). Hence, the KERFIX data are used as constraints of the CO_2 seasonal and interannual interpolation. A direct horizontal advection parameterization is not taken into account in this model since this effect is probably weak on a monthly scale. MLD, S, SST and Chl constraints already contain some informations about the physical properties of the area. Moreover, the eastward circumpolar current partly smoothes the west-east distributions of DIC in the Antarctic Ocean. The expression of the fCO_2 variations with time is thus:

$$(\delta f/\delta t) = (\delta f/\delta t)_F + (\delta f/\delta t)_M + (\delta f/\delta t)_T + (\delta f/\delta t)_B \quad (1)$$

where subscript F, M, T and B represent air-sea exchange, mixing, temperature and biological effects, respectively. The equations of the model are based on month-to-month budget calculations. The contributions of the processes are added to obtain the total CO_2 fugacity variation. Each term of Eq. (1), except the thermal component, is derived from DIC and TA variations. The conversion from DIC and TA variations to fCO_2 variations is done by using Goyet and Poisson (1989) dissociation constants.

The CO_2 air-sea exchange is calculated according to Wanninkhof (1992) and is constrained monthly by the wind speed, the temperature and salinity and the mixed-layer depth variations. The result of this contribution is given in terms of DIC variations. Vertical mixing affects Inorganic Nitrogen (IN), DIC and TA and includes entrainment and mixing. Entrainment of subsurface properties into the surface layer is calculated at each time-step according to Peng *et al.* (1987) as a function of the mixed-layer depth. The mixing effect is constrained by the mixed-layer depth variations and is represented by an input of subsurface properties by entrainment. The thermodynamical effect on fCO_2 is constrained monthly by the variations of temperature and salinity. It is directly calculated using the polynomial of Goyet *et al.* (1993). The biological effect on fCO_2 includes both uptake and mineralization of CO_2 and will be presented as a net effect in the whole study. It is constrained by the variations of chlorophyll concentrations in the mixed layer. It contains the effect on fCO_2 by photosynthesis/respiration and $CaCO_3$ precipitation. Results of the biological effect are expressed in terms of IN variations and translated into carbon and alkalinity by using constant Redfield ratio. The equations in terms of IN, DIC and TA are

presented in the Appendix for each process (see also Louanchi *et al.,* 1996; 1999; Metzl *et al.,* 1999).

The subsurface properties are taken to be invariant. The constraints (T, S, MLD, wind speed, Chl) are linearly interpolated from one month to another because of the daily model time-step. Initial profiles of DIC, TA and IN are taken from the KERFIX 1993 observations. In this model, it is not necessary to define initial surface properties, as the system stabilizes after three years running. However, it is sensitive to subsurface property definitions as pointed out by Peng *et al.* (1987). The depth of the pycnocline is chosen as a reference level for subsurface property concentrations which are derived from 1993 observed profiles. Then the model's spin-up is realized by running it first on year 1990 until stabilization to January 1990 conditions. During the spin-up, atmospheric CO_2 concentration is kept constant at 351.9 ppm (the value observed at Palmer station on average in 1990, Conway *et al.,* 1994). The model is applied to KERFIX station data (presented in Fig. 2) from 1990 to 1995 taking into account an increase of atmospheric CO_2 by 1.2 ppm/yr. No seasonal variation of CO_2 in the atmosphere is taken into account as it is about 1–2 ppm in this area (Ramonet, 1994). Results of this application are presented below.

c. Difference between observed and simulated surface CO_2 distributions in the oceanic mixed-layer

Figure 3 presents available KERFIX DIC, TA and fCO_2 data over the 1990–1995 period together with the results of the model. The standard deviation on the DIC and TA data represents the variability of both parameters in the mixed layer (8 μmol/kg and 5 μeq/kg, respectively). The accuracy of the infra-red continuous method of measurements for pCO_2 is less than 1 ppm (0.3%) (Poisson *et al.,* 1993).

The seasonal DIC variations appear clearly in Figure 3a. Both observed and simulated DIC show an increase of 25 μmol from summer to winter. A difference between data and model of 0.4% is observed for the year 1993, which represents about 8 μmol/kg on average. This difference remains of the same order of magnitude as the measurement accuracy and/or the mixed-layer variability. DIC measured variations are well reproduced by the model. DIC seasonal variation reflects a Net Community Production (NCP) of about 30 gC/m2/yr, which is approximately half of the primary production at KERFIX (Pondaven *et al.,* 1998). Therefore, an *f*-ratio of about 0.5 can be derived for this area for spring–summer period and is in good agreement with earlier studies (Minas and Minas, 1992). The observed seasonal or interannual changes in alkalinity remain low (Fig. 3b), following more or less the surface salinity distributions (Fig. 2d). The range of TA values is well reproduced by the model with an amplitude of variations about 8 μmol. However, the modeled TA seasonal variations are not in phase with the observed ones. As the KERFIX area is dominated by dinoflagellates and diatoms, phytoplankton species and only a few coccolithophorids are present there, the $CaCO_3$ precipitation is probably overestimated in the model (see Appendix). However, TA variations are low at KERFIX and hence, have a small impact on fCO_2 distributions as we will see below. The oceanic simulated and

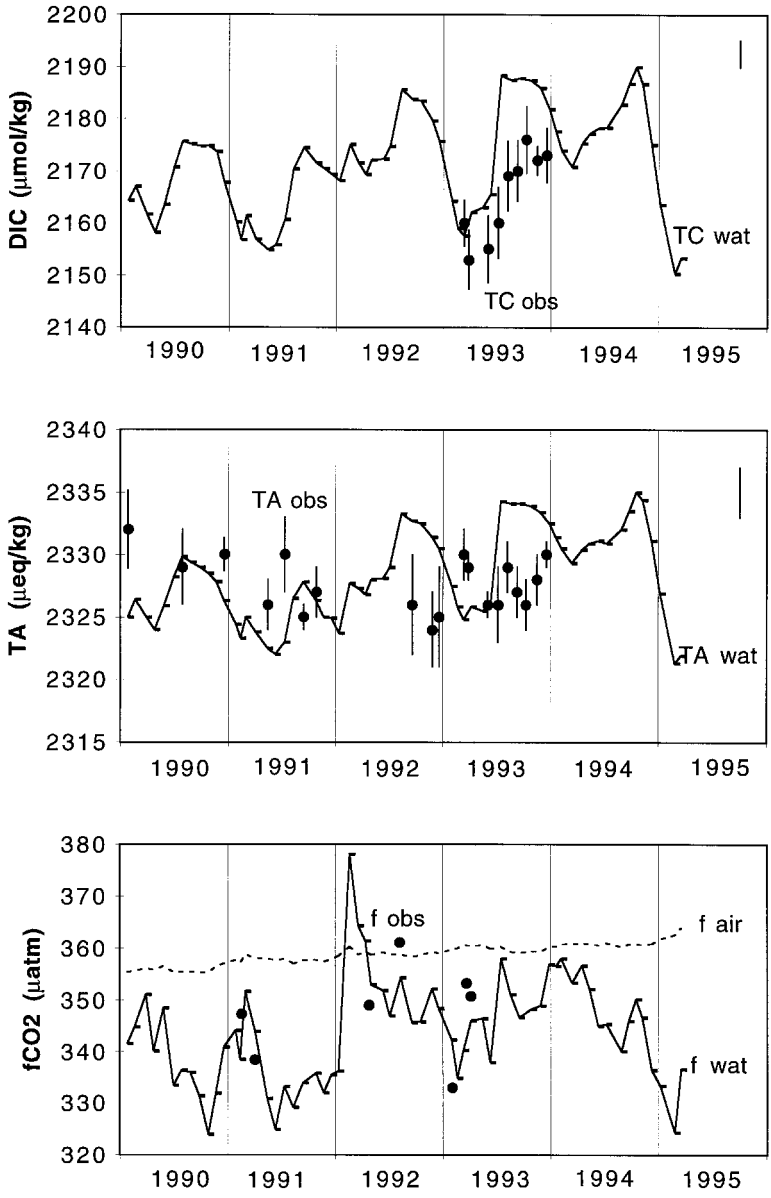

Figure 3. (a) Simulated surface DIC (line) and observed DIC (black circles) at KERFIX station for the 1990–1995 period. The error bars represent the DIC variability in the mixed-layer depth and the bar in the right-upper part of the panel the measurements accuracy. (b) Simulated surface alkalinity (line) and observed TA (black circles) same location and period. The error bars represent the TA variability in the mixed-layer depth and the bar in the upper right-part of the panel the measurements accuracy. Note that the TA variability in the mixed layer appears important because the scale is stretched. (c) Simulated sea surface fCO_2 (line), fCO_2 in the air (dotted line), and observed fCO_2 (black circles) from the MINERVE cruises at KERFIX between 1990–1995.

measured fCO_2 in the mixed layer values at the KERFIX site are presented in Figure 3c. The simulated values of fCO_2 are always lower than the atmospheric CO_2 level, except in February 92. This is due to the abrupt increase in the mixed-layer depth and temperature (Fig. 2b, c). KERFIX is therefore a CO_2 sink during the whole period investigated. A good agreement between sporadic fCO_2 data (from underlying continuous measurements, see Fig. 3 legend) and model results is obtained. Seasonal variations of fCO_2 are in the range of 10 to 30 µatm depending on the year considered.

Seasonal variations of DIC and TA are comparable to those reported at the HOT station in the subtropical Pacific (Winn *et al.,* 1994), and are two times lower than those observed in the subtropical Atlantic Ocean at the BATS station (Bates *et al.,* 1996). At the KERFIX site, Chl is always less than 1.4 mg/m^3 during the spring–summer period, reflecting low primary productivity. As a consequence, the gradient between surface and subsurface DIC and TA is not strong enough to induce an important increase from summer through winter following the mixed-layer depth increase. This result is similar to the situation observed at the oligotrophic site HOT (typical subtropical conditions). On the contrary, the BATS site reports higher primary production levels (about 140 gC/m^2/yr, Michaels *et al.,* 1994), and stronger seasonal DIC, TA and fCO_2 signals. In spite of the HNLC conditions prevailing at KERFIX site, it has been shown that the POOZ area is one of the major sinks for biogenic silicon (Tréguer *et al.,* 1995). This fact suggests that the biology may also be efficient in removing the surface CO_2 to the bottom layers, leading to its storage in deep waters. The quantified impact of the biological processes on the surface carbon cycle at KERFIX station is investigated in the next section.

4. Processes controlling surface oceanic fCO_2 seasonal changes

To evaluate the relative importance of each process involved in surface carbon variations at seasonal time scales, the results of the simulation obtained between the years 1990 and 1995 (Fig. 3) were used to calculate a climatological average of the annual cycle. The mean annual distribution of fCO_2 and air-sea CO_2 fluxes are presented in Figures 4a and b respectively. The effect on fCO_2 variations of each process involved in the CO_2 changes in the mixed layer (in %) were integrated over four seasons: summer (December through February), fall (March through May), winter (June through August) and spring (September through November). The seasonal impact of all processes (Air-Sea flux, biological activity, mixing and temperature) are shown in Figure 4c and Table 1.

fCO_2 increases slightly in summer time (Fig. 4a) following the temperature increase (Fig. 2c). An important biological contribution of the order of 40% is balanced by the CO_2 flux from the atmosphere as well as the temperature increase. In fall fCO_2 is decreasing following the decrease of the temperature. The rest of the year fCO_2 variations are low because during winter and spring, the contributions of the processes approximately cancel each other. The KERFIX site is a sink throughout the year with a value of about -2 mol/m^2/yr (Fig. 4b). This sink is related to the air-sea fCO_2 gradient (ΔfCO_2) which is also negative throughout the year (Fig. 4a). The intensity of the CO_2 fluxes depends on the

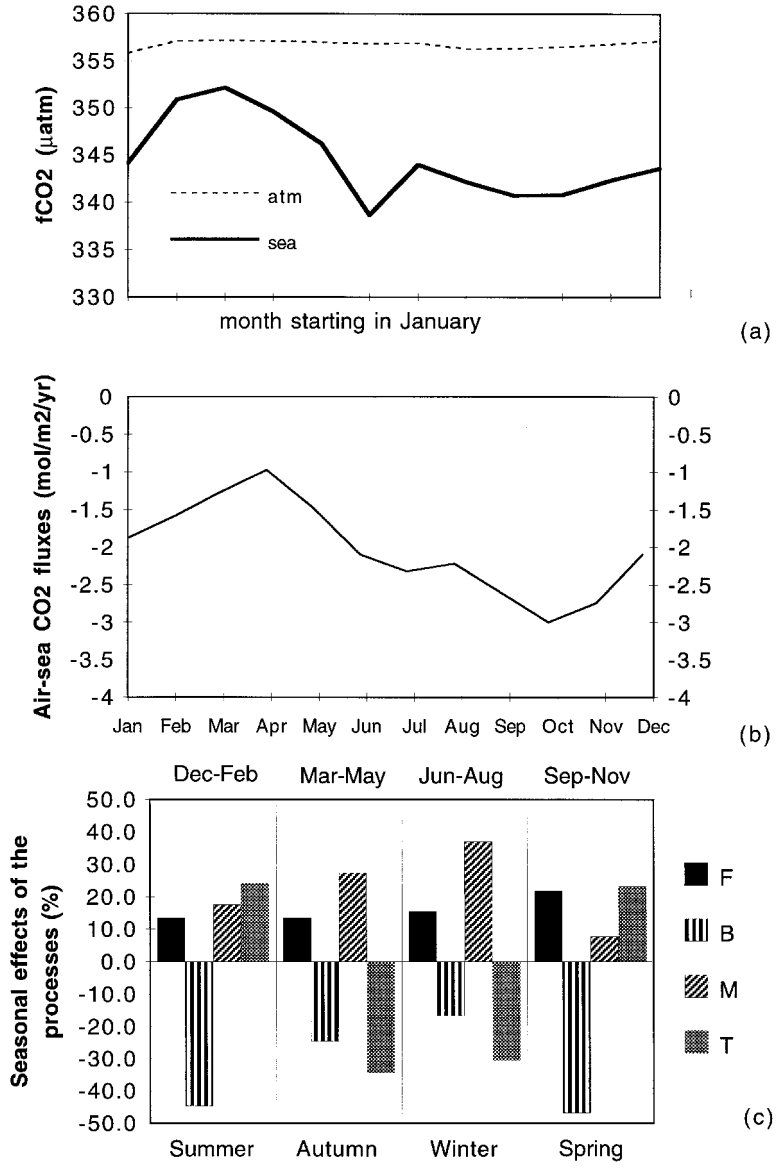

Figure 4. (a) Oceanic (black line) and atmospheric (dotted line) fCO_2 annual cycles obtained as the mean year for 1990–1995 simulation at KERFIX station. (b) Air-sea CO_2 fluxes annual course obtained as the mean year for 1990–1995 simulation at KERFIX station. (c) Seasonal effects of the processes on fCO_2 variations over the period 90–95 at KERFIX station. F is related to the air-sea CO_2 flux effect on fCO_2, B is related to the biological activity, M is related to both the entrainment/detrainment effect and the mixing effect, and T is related to thermodynamics.

Table 1. Effects of air-sea CO_2 fluxes (F), biological CO_2 uptake (B), mixing processes (M) and temperature (T) on fCO_2 integrated over four seasons: summer (Dec.– Feb.), fall (Mar.–May), winter (Jun.–Aug.) and spring (Sep.–Nov.). Absolute sum of all processes in one season represents the total variation of fCO_2. It is used to estimate the contribution percentage of each process on fCO_2 variations on a seasonal basis (see Fig. 4c).

Period	F (µatm)	B (µatm)	M (µatm)	T (µatm)
Dec.–Feb.	+12.1	−39.9	+15.9	+21.7
Mar.–May	+08.0	−14.8	+16.3	−20.5
Jun.–Aug.	+09.2	−09.9	+22.0	−18.1
Sep.–Nov.	+14.3	−30.5	+05.0	+15.8

wind-speed values, from which the calculations of the CO_2 exchange coefficient are derived. The sink is maximal around October (Fig. 4b) due to the most negative value of ΔfCO_2 in early spring (Fig. 4a), and the high wind speeds observed between September and November (Fig. 2a). The lower sink is found in March–April when ΔfCO_2 is the lowest (with values around –15 µatm) and the wind speeds are lower than the five year mean value of 11.4 m/s.

A striking observation is the high biological activity contribution during spring and summer (Fig. 4c), to which about 45% of the total fCO_2 variation can be attributed (see Table 1). The mixing effect is maximized during the winter, to which about 40% of the fCO_2 variations can be attributed. According to the season, the thermodynamic contribution can be either positive or negative ranging from 24 to 35% of the fCO_2 variation throughout the year. The level of mixed-layer DIC is low in summer and high in winter (Fig. 3a) as a result of biological uptake and low mixing, respectively. However, for the fCO_2 budget, the SST increase effect during spring and summer partly compensates for the biological uptake effect, whereas its decrease is strong enough to compensate for the effect of the mixing in fall (Table 1). Except during spring when wind speeds are at their peak, the air-sea exchange weakly affects fCO_2 variations. Summing the budgets on fCO_2 variations over one year shows contributions varying from 15% for the air-sea flux to 34% for the biological activity. The thermodynamical process represents 29% of fCO_2 variations and the mixing is in the order of 20%. Although KERFIX is a HNLC system, the biological activity plays an important role on its fCO_2 level.

5. Interannual surface oceanic fCO_2 variations

At KERFIX, at interannual time-scales, the fCO_2 and DIC variability can be explained by the strong variabilities of hydrological and biological parameters (used here as constraints of the model, Fig. 2). These constraints affect the physical and biogeochemical processes interannual variations.

a. Method of analysis

The impact of each process on interannual fCO_2 variations are quantified by performing a series of simulations. The fCO_2 result based on the combination of all processes is called TFBM (Temperature, Fluxes, Biology and Mixing, Fig. 5a). TFBM also includes the atmospheric CO_2 increase in the air-sea CO_2 fluxes contribution. The second fCO_2 result obtained without including biological activity is called TFM. In the latter run, DIC stabilizes at the subsurface concentration and the seasonal cycle in fCO_2 is mainly due to the temperature annual cycle. The difference between TFBM and TFM, therefore, gives the biological impact B on fCO_2 variations. The run called TF (Fig. 5b) includes thermodynamical and air-sea exchange effects on fCO_2. The impact of the mixing M on fCO_2 variations is thus calculated as the difference TFBM-B-TF. In this model, the mixing effect is proportional to the DIC surface-subsurface gradient. A high mixing effect is thus expected when the biological uptake of DIC is strong. When only the thermodynamical effect is used the run is called T (Fig. 5c). The impact of air-sea exchange on fCO_2 variations F is given by the difference TFBM-T-M-B. Finally, the thermodynamical effect is calculated as the difference TFBM-F-M-B. The annual integrated effects of each process are presented in Figure 5d and Table 2.

b. Results

The TFM simulation shows that the KERFIX site is converted into a CO_2 supersaturation of +9 μatm when the biological activity is suppressed. This means that the biological activity causes a decrease of the fCO_2 signal by a mean of 18 μatm on average (Table 2). The largest differences between TFM and TFBM occurred during the summer period with values ranging from 20 to 45 μatm depending on the year (Fig. 5a). The mixing contribution varies between 10 and 55 μatm depending on the season of the year considered; its largest value occurring during autumn and winter. Because KERFIX is a sink area, the air-sea gas exchange adds CO_2 to the surface layer. Its contribution to interannual fCO_2 variations lies from 12 to 30 μatm depending on the year (Table 2). Finally, the thermodynamical effect decreased the CO_2 signal by a 15 μatm mean over the five years (Fig. 5c). It is worth noting that at interannual time scales biological activity plays a role as important as the thermodynamical processes on fCO_2 variability.

Net integrated contribution to fCO_2 variations by every process (in terms of percentages) are presented in Figure 5d. B decreases fCO_2 by 14 to 30% depending on the year. Its largest contribution, occurring in 1991, is clearly related to the highest levels of chlorophyll (Fig. 2e). M increases fCO_2 by 20 to 45%. The maximal value occurred in 1990 when the DIC surface-subsurface gradient was maximal (Fig. 3a). T decreases fCO_2 on an annual basis, with values ranging between 4 to 29%. Its most important contribution occurred in 1994 when the temperatures were the lowest. F appears to affect strongly the interannual fCO_2 variations with an annual mean value ranging from 17 to 35%. Quantitatively, over the five-year period, the air-sea exchange is responsible for $(+29 \pm 11)$% of the interannual fCO_2 variability, the biological pump for (-21 ± 4)%, the mixing for $(+31 \pm 6\%)$

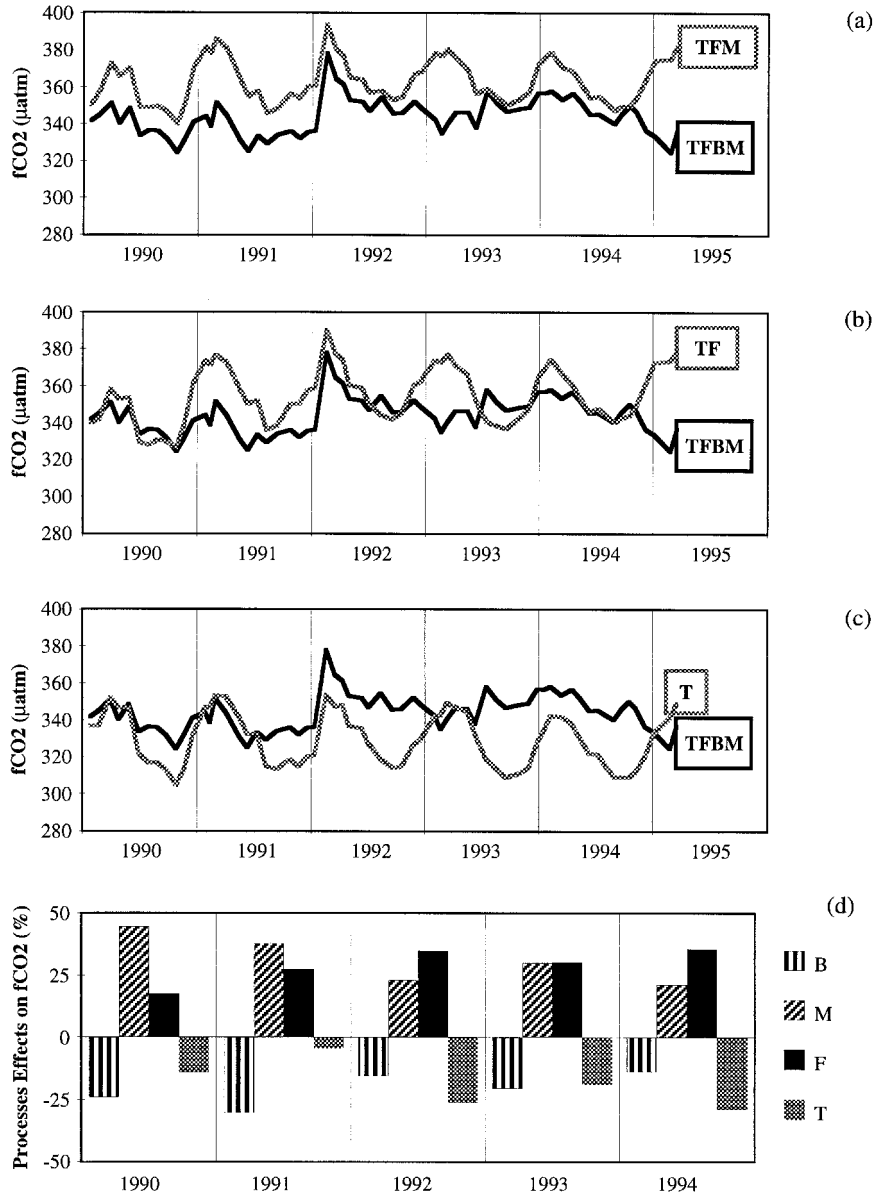

Figure 5. Simulated oceanic fCO_2 for several runs at KERFIX site for the 1990–1995 period: (a) TFBM is the run which includes all the processes involved in fCO_2 variations. In the TFM run, the biological effect is suppressed. (b) In the TF run, mixing and biological effect are suppressed. (c) In the T run, only the thermodynamical effect is acting on fCO_2 variations. (d) Annual impact of each process on fCO_2 variations (in percentage). F is related to the air-sea CO_2 flux effect on fCO_2, B is related to the biological activity, M is related to both the entrainment/detrainment effect and the mixing effect, and T is related to thermodynamics.

Table 2. Effects of air-sea CO_2 fluxes (F), biological CO_2 uptake (B), mixing processes (M) and temperature (T) on fCO_2 annually integrated. Absolute sum of all processes over one year represents the total variation of fCO_2. It is used to estimate the contribution percentage of each process on fCO_2 variations on an annual basis (see Fig. 5d).

Year	F (μatm)	B (μatm)	M (μatm)	T (μatm)
1990	+12.8	−17.6	+32.7	−10.4
1991	+25.1	−27.6	+34.5	−04.0
1992	+29.4	−13.3	+19.4	−22.3
1993	+27.5	−18.8	+27.2	−17.2
1994	+30.5	−12.0	+18.2	−24.8

and the thermodynamic process for $(-19 \pm 3)\%$. The dominating processes in interannual fCO_2 variabilities are the effects from the mixing and the air-sea exchange. However, a caution has to be made according to the fact that the nonlinearity of the processes and the possible feedback of one process on another are not taken into account in this way of estimating the contribution of each process on fCO_2 variations. Nevertheless, at this time scale the air-sea exchange contribution to the CO_2 appears to be most variable from one year to another. This interannual variability seems to be highly correlated to the high wind-speed variability (Fig. 2a) and in a lesser way to the changes in air-sea CO_2 gradients. The air-sea CO_2 exchange depends on both air-sea CO_2 gradient and wind speed variability. Thus its effect on fCO_2 variations contains atmospheric conditions as well as oceanic parameter changes. We will see below how the air-sea CO_2 flux is affected by natural and anthropogenic CO_2 changes.

6. Impact of atmospheric CO_2 increase on fCO_2 and air-sea CO_2 exchange

The monthly air-sea CO_2 fluxes between 1990 and 1994 are presented in Figure 6a. Annual integrated values always show a sink (represented by negative values). The intensity of the sink is highly variable at an estimated interannual variability of 40%. The interannual variation of the sink seems to be correlated to the wind-speed anomalies (presented on the same figure). Resulting from the most intense biological activity, the largest CO_2 sink occurred in 1991 (Figs. 5a and 5b). It is also during 1991 that the wind speed presents the most positive anomaly. The weakest CO_2 sink occurred in 1992 as a result of the big impact of the air-sea exchange on fCO_2 and the weak biological contribution.

To observe a trend of increase in surface fCO_2 due to atmospheric CO_2 increase, more DIC and/or fCO_2 data than those obtained at KERFIX should be necessary. To separate anthropogenic CO_2 effects from natural variability, two simulations are performed. The first simulation is the one which takes into account all the processes (TFBM) with an atmospheric CO_2 increase of 1.2 ppm/year (mean CO_2 increase at Palmer Station, Conway *et al.,* 1994). The second one includes all the processes except the atmospheric CO_2

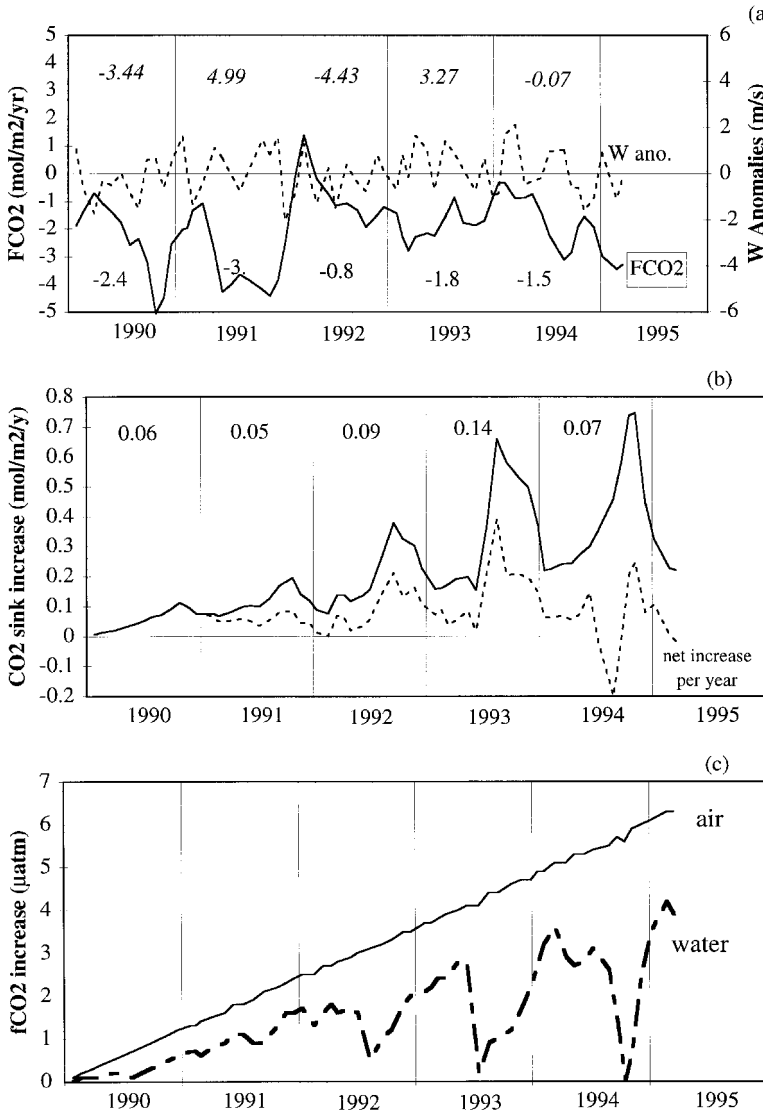

Figure 6. (a) Air-sea CO_2 fluxes over the 1990–1995 period as a result of the simulation. The values indicate the annual mean flux on each year. A negative flux indicates that the ocean is a CO_2 sink for the atmosphere. The values in the lower part of the panel for each year represent the annual accumulated CO_2 flux in mol/m^2/yr. The dotted line represents the anomalies of wind-speeds at KERFIX station for the 1990–1995 period. Wind-speed anomalies are referred to the wind speed five years climatology (1990–1994). The values in the upper part of the panel are the annual integration of the wind-speed anomalies. (b) Air-sea CO_2 sink increase in mol/m^2/yr obtained from the difference between a steady state run of the model (xCO_2 in the air is a constant: 351.9 ppm) and a "perturbed" run of the model (with xCO_2 = 351.9 ppm + 1.2 ppm/yr. The increase rate of atmospheric CO_2 is obtained from Conway *et al.,* 1994). (c) fCO_2 increase (in µatm) obtained by the same method in surface waters (dashed line) and air (prescribed) over the same period at KERFIX station.

increase from 1990 to 1995 and is thus conducted with a constant CO_2 molar fraction of 351.9 ppm. The difference between both simulations, therefore, quantifies the impact of atmospheric CO_2 increase on sea-surface fCO_2 and air-sea CO_2 exchange.

This comparison shows an increase of the CO_2 sink at KERFIX from 1990 to 1995 (Fig. 6b). The total CO_2 anthropogenic uptake increases between 1990 and 1991 by about 6% and reaches 10% between 1992 and 1994. Figure 6c shows the atmospheric fCO_2 increase and its effect on oceanic fCO_2. The oceanic fCO_2 signal followed the atmospheric increase only during the first years of the simulation. Larger differences between atmospheric and oceanic signals appeared after 1992. Indeed, the oceanic fCO_2 increase was reduced from 0.70 to 0.38 µatm/yr after 1992. The impact of the CO_2 atmospheric increase on oceanic fCO_2 at KERFIX differs from that observed in the NW Pacific (also a sink area) (Inoue *et al.,* 1995). In the NW Pacific the oceanic CO_2 increase rate followed the atmospheric rate. The sink increase at KERFIX can be explained as follows: due to a 6 µatm total atmospheric CO_2 increase over 5 years (i.e., 1.7%) (Fig. 6c), the oceanic fCO_2 increased by 2.7 µatm (0.8%) in five years (two times lower than the atmospheric increase). In other words, the increase in the surface ocean is lower than the atmospheric CO_2 increase. Consequently the air-sea CO_2 gradient increases due to the atmospheric CO_2 increase. The same result was found for the Indian Subtropical gyre (Metzl *et al.,* 1999).

Another aspect is worth pointing out. In this study, the surface layer is enhanced by CO_2 from the atmosphere because the KERFIX station is a CO_2 sink. The CO_2 enhancement of the surface layer therefore induces a decrease in the CO_2 gradient between the surface and the subsurface layers, (the latter taken to be invariant in the model). Thus, the oceanic uptake of CO_2 from the atmosphere induces a decrease in time of the mixing contribution in the model. Of course, in reality, the CO_2 pumped from the atmosphere is not all accumulating in the surface layers of the ocean, but is transferred by vertical advection and biological fluxes into the water column. If we consider that the increase of subsurface CO_2 would be less than in the surface layer, thus the effect calculated by the model would be a low estimate of the sink increase. However some uncertainties in these model results have to be underlined. In this estimate, we took Wanninkhof's (1992) relationship between piston velocity and wind speeds to calculate the air-sea gas exchange. The use of one relationship or another is still a matter of debate and induces a significant difference in the CO_2 fluxes estimates (Wanninkhof, 1992). Moreover, the effect of atmospheric pressure variability on fCO_2 in the air or the seasonality of the latter were not studied. Indeed, if fCO_2 seasonality in the air is only about 1 ppm in this area (Ramonet, 1994), atmospheric pressure present high variability at seasonal and interannual scales and may significantly change our estimate of the sink increase.

Extending this minimal effect to the entire POOZ area (approximately 25.10^6 km^2 between 50 and 60S) would induce a potential increase of the CO_2 sink by $+0.02$ GtC/yr. Although this impact is weak, it represents about 10% of the total Arctic sea CO_2 uptake (data based estimate, Tans *et al.,* 1990).

7. Conclusions

The five-year KERFIX time series provide for the first time insight into the seasonal and interannual evolution of hydrological and geochemical parameters in an open area of the Southern Ocean. In this region, all parameters show marked seasonal signals due to extreme weather conditions, whereas the carbon system parameters (DIC and TA) present reduced variability which can be compared to that of oligotrophic areas. The application of a 1D model gives us a better understanding of the processes controlling the seasonal and interannual variations of CO_2 in the POOZ subregion of the Southern Ocean. The seasonal evolution of CO_2 appears to be mainly affected by biological and thermodynamic changes. The interannual variability is mainly controlled by wind speeds and mixed-layer depth. The latter may be of the same magnitude as seasonal changes of the mixed-layer depth (Park *et al.,* 1999). The KERFIX site was a sink all year round over the period investigated with an average influx of 2 mol/m^2/yr.

Even if the POOZ is considered as HNLC, the biological pump of CO_2 acts intensively at both seasonal and interannual time scales. This local result based on *in situ* measurement extrapolation complies with recent observations in the Weddel gyre (Hoppema *et al.,* 1995). The interannual variability in air-sea CO_2 exchange in the Southern Ocean is mainly due to the interannual changes of climatic conditions, which appear to affect the oceanic uptake by 50% yearly. The extrapolation of KERFIX air-sea CO_2 annual fluxes to the whole POOZ area results in a variation of the oceanic uptake from 0.2 GtC/yr in 1992 to 0.9 GtC/yr in 1991. This strong variability may affect the global carbon budget and could be responsible for an important part of the uncertainties of the global oceanic uptake. The model quantified an increase of oceanic fCO_2 about half of that observed in the atmosphere. This effect implies a potential increase of oceanic CO_2 sink by 0.07 mol/m^2/yr. Moreover, extending this result to the entire POOZ area increases the oceanic CO_2 sink by 0.02 GtC/yr. This additional sink is weak compared to the large seasonal and interannual variabilities linked to natural processes in the ocean. However, one can expect that it may contribute to the decrease of the atmospheric CO_2 growth rate, as revealed from recent studies for the nineties (Conway *et al.,* 1994; Keeling *et al.,* 1995). This result complies with the recent assumptions that the ocean CO_2 uptake is increasing (Keeling *et al.,* 1995; Francey *et al.,* 1995).

To analyze the CO_2 uptake variation on longer time scales, one has to take into account the circulation changes in the Southern Ocean as revealed by the 3D-OGCM's predictions (Sarmiento and Le Quéré, 1996). As a matter of fact, the changes of the circulation will induce a variation in biological uptake of CO_2 and thus in the processes of invasion of surface CO_2 into the deep oceanic layers.

Acknowledgments. Thanks to the support of the Institut Français de la Recherche et la Technologie Polaires, the CNRS (Centre National de la Recherche Scientifique Française) and the JGOFS-France program for the Southern Ocean KERFIX was possible. We thank the captains and crew of the ship "*La curieuse*" for their continuous help on board. KERFIX data sets could not exist without the participation of eight young volunteers who sampled the data in extreme weather conditions for five

years. We are grateful to Dr. Catherine Jeandel who was responsible for the KERFIX station between 1993 to 1995 and to Elvis Gjata for the data processing. The chlorophyll data were kindly made available by Dr. Michel Fiala. We thank Christian Brunet and Bernard Schauer for supervising the sampling and measurements of KERFIX geochemical data in Paris as well as on Kerguelen Island. Dr. Raymond G. Najjar and two anonymous reviewers are acknowledged for their comments which helped to make the manuscript clearer.

APPENDIX

Model description

a. Air-sea Exchange effect on fCO_2 variations

The air-sea exchange of CO_2 is calculated according to Wanninkhof (1992). At each time step the flux at the air-sea interface (FCO_2) is calculated as a function of the wind speed, the temperature and the salinity and translated into a change of dissolved inorganic carbon (DIC):

$$F_{CO_2} = K * S_{CO_2} * \Delta fCO_2$$

where K is the piston velocity and is a quadratic function of the wind-speed, SCO_2 is the CO_2 solubility computed from temperature and salinity data (Weiss, 1974) and ΔfCO_2 the air-sea fCO_2 difference. The air-sea exchange affects only DIC in the mixed-layer depth Z and the variations of DIC are computed at each time-step as follows:

$$\delta DIC/\delta t = F_{CO_2}/Z$$

The variations of DIC associated with the air-sea CO_2 exchange is used to calculate fCO_2 changes expressed as $(\delta f/\delta t)_F$ in Eq. (1) by using Goyet and Poisson (1989) dissociation constants.

b. Mixing effect on fCO_2 variations

The mixing effect is estimated as the entrainment described in Peng *et al.* (1987) and the input of subsurface properties into the surface layer by the general Southern Ocean upwelling. These processes affect inorganic nitrogen (IN), total alkalinity (TA) and dissolved inorganic carbon (DIC) and are dependent on the mixed-layer depth and the surface-subsurface gradient of the geochemical properties. Changes due to the mixing effect are calculated according to:

$$\delta G/\delta t = \delta Z/\delta t * (G_b - G_s)/Z + w * (G_b - G_s)/Z$$

where G is the geochemical property, G_b and G_s are the concentrations of G in the subsurface and surface boxes, respectively, Z is the mixed-layer depth and w is the vertical velocity (taken at 40 m/yr according to Gordon and Huber, 1990). Subsurface concentrations are taken from KERFIX data and are 2215 µmol/kg for DIC, 2340 µeq/kg for TA and 30 µmol/kg for IN. It represents the concentrations of the species at the pycnocline depth. The variations of TA and DIC according to the vertical mixing processes give fCO_2 changes expressed as $(\delta f/\delta t)_M$ in Eq. (1).

c. Biological effect on fCO_2 variations

The biological impact on fCO_2 variations in the model is developed with sensitivity tests in Louanchi *et al.* (1996). Here, the main equations showing the chlorophyll constraints on the biological activity are presented. Most of the parametrizations are adapted from Taylor *et al.* (1991). The variation of chlorophyll biomass is expressed as

$$\delta\mathrm{Chl}/\delta t = (U - Q) * \mathrm{Chl}$$

where U is the growth of the phytoplankton and is expressed as a Michaelis-Menten function of the nutrient IN: $U = U_m * (IN/(IN + K_m))$. In this expression U_m is the maximal growth rate of 0.52 d^{-1} (according to Minas and Minas, 1992) and K_m is the half-saturation constant of the growth on IN (0.2 μmol/kg). U is calculated at each time-step. Q represents the total loss (as grazing, mortality or respiration). In this model, it is deduced from U and Chl changes in the surface layer following the equation:

$$Q = U - \delta \ln(\mathrm{Chl})/\delta t.$$

Part of the production is regenerated in the mixed layer. Finally the variation of IN with time is

$$\delta IN/\delta t = -(U - R_s * Q) * \mathrm{Chl} * \mathrm{N/Chl}.$$

In the latter expression, R_s represents the removal factor in the surface layer taken at 0.5 according to Olson (1980) and Minas and Minas (1992) for the Indian sector of the Southern Ocean. N/Chl is the nitrogen chlorophyll ratio (7.5 in this study).

The exported production is expressed in carbon units as:

$$P_{\mathrm{exp}} = (1 - R_s) * Q * \mathrm{Chl} * \mathrm{C/Chl}$$

where C:Chl is the Carbon to chlorophyll constant ratio of 45. We consider that 20% of the exported production is $CaCO_3$ (1 inorganic particulate matter vs. 4 organic particulate matter, Broecker and Peng, 1982). Finally the total biological effect on DIC and TA is:

$$(\delta\mathrm{DIC}/\delta t)_B = (\delta IN/\delta t) * (6/1) - 0.2 * P_{\mathrm{exp}}$$

$$(\delta\mathrm{TA}/\delta t)_B = -(\delta IN/\delta t) * (1/1) - 2 * (0.2 * P_{\mathrm{exp}})$$

These variations give the fCO_2 changes at each time-step expressed as $(\delta f/\delta t)_B$ in Eq. (1).

d. Thermodynamical effect on fCO2 variations

Finally the thermodynamical effect on $fCO2$ variations is directly computed at each time step following the polynomial of Goyet *et al.* (1993). This calculation gives $(\delta f/\delta t)_T$ in Eq. (1).

REFERENCES

Bates, N. R., A. F. Michaels and A. H. Knap. 1996. Seasonal and interannual variability of carbon dioxide species at the U.S. JGOFS Bermuda Atlantic Time-Series Study (BATS) site. Deep-Sea Res., *43,* 347–383.

Boutin, J. and J. Etcheto. 1996. Consistency of Geosat, SSM/I, and ERS-1 global surface wind speeds—Comparison with *in situ* data. J. Atmos. Ocean. Technol., *13,* 183–197.

Broecker, W. S. and T.-H. Peng. 1982. Tracers in the Sea, Eldigio Press, Lamont-Doherty Geological Observatory, Palisades, NY, 690 pp.

Conway, T. J., P. P. Tans, L. S. Waterman, K. W. Thoning, D. R. Kitzis, K. A. Masarie and N. Zhang. 1994. Evidence for interannual variability of the carbon cycle from the National Oceanic and Atmospheric Administration/Climate Monitoring and Diagnostics Laboratory Global Air Sampling Network. J. Geophys. Res., *D99,* 22831–22855.

DOE. 1991. Handbook of methods for the analysis of the various parameters of the carbon dioxide system in sea water, A. G. Dickson and C. Goyet, eds., ORNL/CDIAC.

Edmond, J. M. 1970. High precision determination of alkalinity and total CO_2 of sea water by potentiometric titration. Deep-Sea Res., *17,* 737–750.

Francey, R., P. P. Tans, C. E. Allison, I. G. Enting, J. W. C. White and M. Trolier. 1995. Changes in oceanic and terrestrial carbon uptake since 1982. Nature, *373,* 326–330.

Gordon, A. L. and B. A. Huber. 1990. Southern Ocean winter mixed layer. J. Geophys. Res., *C95,* 11655–11672.

Goyet, C., F. J. Millero, A. Poisson and D. K. Shafer. 1993. Temperature dependance of CO_2 fugacity in seawater. Mar. Chem., *44,* 205–219.

Goyet, C. and A. Poisson. 1989. New determination of carbonic acid dissociation constants in seawater as a function of temperature and salinity. Deep-Sea Res., *36,* 1635–1654.

Hoppema, M., E. Fahrbach, M. Schröder, A. Wisotzki and H. J. W. de Baar. 1995. Winter-summer differences of carbon dioxide and oxygen in the Weddel Sea surface layer. Mar. Chem., *51,* 177–192.

Houghton, J. T., L. G. Meira Filho, B. A. Callander, N. Harris, A. Kattenberg and K. Maskell, eds. 1996. Climate change 1995—The science of climate change: Contribution of working group I to the second Assessment Report of the Intergovernmental Panel on Climate Change, Cambridge Univ. Press, Cambridge.

Inoue, H. Y., H. Matsueda, M. Ishii, K. Fushimi, M. Hirota, I. Asanuma and Y. Takasugi. 1995. Long-term trend of the partial pressure of carbon dioxide (pCO_2) in surface waters of the Western North Pacific, 1984–1993. Tellus, *47B,* 391–413.

Jacques, G. 1989. Primary production in the open Antarctic Ocean during the Austral summer. A review. Vie et Milieu, *39,* 1–17.

Jacques, G. and M. Minas. 1981. Production primaire dans le secteur Indien de l'océan Antarctique en fin d'été. Oceanol. Acta, *4,* 33–41.

Jeandel, C., D. P. Ruiz-Pino, E. Gjata, A. Poisson, C. Brunet, E. Charriaud, F. Dehairs, D. Delille, M. Fiala, C. Fravalo, J. C. Miquel, Y.-H. Park, S. Razouls, B. Quéguiner, B. Schauer and P. Tréguer. 1999. KERFIX, a permanent time series station in the Southern ocean: A presentation. J. Mar. Syst. (in press).

Keeling, C. D. 1973. The carbon dioxide cycle: Reservoir models, to depict the exchange of atmospheric carbon dioxide with the oceans and land plants, *in* Chemistry of the Lower Atmosphere, S. Rasool, ed., Plennum Press, NY, 251–329.

Keeling, C. D., S. C. Piper and M. Heimann. 1989. A three-dimensional model of atmospheric CO_2 transport based on observed winds, 4, Mean annual gradients and interannual variations, *in* Aspects of Climate Variability in the Pacific and the Western Americas, Geophys. Monogr. 55, D. H. Peterson, ed., AGU, Washington D.C., 305–363.

Keeling, C. D., T. P. Whorf, M. Wahlen and J. van der Plicht. 1995. Interannual extremes in the rate of rise of atmospheric carbon dioxide since 1980. Nature, *375,* 666–670.

Liss, P. and L. Merlivat. 1986. Air-sea exchange rates, introduction and synthesis, *in* The Role of Air-Sea Exchange in Geochemical Cycling, P. Buat-Ménard, ed., NATO/ASI Series, D. Reidel, Dordrecht, 113–127.

Louanchi, F. 1995. Etude des variabilités spatio-temporelles de fCO_2 à la surface de l'océan Indien: Processus et quantification. Doctorat de l'Université de Paris 6, Ph.D. dissertation, 234 pp.

Louanchi, F., M. Hoppema, D. C. E. Bakker, A. Poisson, M. H. C. Stoll, H. J. W. de Baar, B. Schauer, D. P. Ruiz-Pino and D. Wolf-Gladrow. 1999. Modelled and observed sea surface fCO_2 in the Southern Ocean: a comparative study. Tellus (in press).

Louanchi, F., N. Metzl and A. Poisson. 1996. Modelling the monthly sea surface fCO_2 fields in the Indian Ocean. Mar. Chem., *55,* 265–279.

Metzl, N., F. Louanchi and A. Poisson. 1999. Seasonal and Interannual variations of sea surface carbon dioxide in the Subtropical Indian Ocean. Mar. Chem. (in press).

Metzl, N., A. Poisson, F. Louanchi, C. Brunet, B. Schauer and B. Brĕs. 1995. Spatio-temporal distributions of air-sea fluxes of CO_2 in the Indian and Antarctic Oceans. Tellus, *47B,* 56–69.

Michaels, A. F., A. H. Knap, R. L. Dow, K. Gundersen, R. J. Johnson, J. Sorensen, A. Close, G. A. Knauer, S. E. Lohrenz, V. A. Asper, M. Tuel and R. Bidigare. 1994. Seasonal patterns of ocean biogeochemistry at the U.S. JGOFS Bermuda Atlantic time-series study site. Deep-Sea Res. I, *41,* 1013–1038.

Minas, H. J. and M. Minas. 1992. Net community production in "High Nutrient—Low Chlorophyll" waters of the tropical and Antarctic oceans: grazing vs. iron hypothesis. Oceanol. Acta, *15,* 145–162.

Murphy, P. P., R. A. Feely, R. H. Gammon, D. E. Harrison, K. C. Kelly, and L. S. Waterman. 1991. Assessment of the air-sea exchange of CO_2 in the South Pacific during austral autumn. J. Geophys. Res., *C96,* 20455–20465.

Olson, R. J. 1980. Nitrate and ammonium uptake in Antarctic waters. Limnol. Oceanogr., *25,* 1064–1074.

Park, Y.-H., E. Charriaud, D. P. Ruiz-Pino and C. Jeandel. 1999. Seasonal and Interannual variability of the mixed-layer properties and steric height at Station Kerfix, southwest off Kerguelen. J. Mar. Syst. (in press).

Peng, T.-H., T. Takahashi, W. S. Broecker, and J. Olafsson. 1987. Seasonal variability of carbon dioxide, nutrients and oxygen in the northern North Atlantic surface water: observations and a model. Tellus, *39B,* 439–458.

Poisson, A., N. Metzl, C. Brunet, B. Schauer, B. Brès, D. P. Ruiz-Pino and F. Louanchi. 1993. Variability of sources and sinks of CO_2 in the Western Indian and Southern Oceans during the year 1991. J. Geophys. Res., *98,* 22759–22778.

Poisson, A., N. Metzl, X. Danet, F. Louanchi, C. Brunet, B. Schauer, B. Brès, and D. P. Ruiz-Pino. 1994. Air-sea CO_2 fluxes in the Southern Ocean between 25E and 85E, *in* The Polar Oceans and Their Role in Shaping the Global Environment, Geophys. Monogr. *85,* O. M. Johannessen *et al.,* ed., AGU, Washington, D.C., 273–284.

Poisson, A., B. Schauer and C. Brunet. 1990. MD53/INDIGO 3, *in* Les rapports des campagnes à la mer. 87 (02), Publ. Mission Rech. des Terres Austral. et Antarc. Fr., Paris, 269 pp.

Pondaven, P., C. Fravalo, D. P. Ruiz-Pino, P. Tréguer, B. Quéguiner and C. Jeandel. 1999. Modelling the silica pump in the Permanently Open Ocean Zone (POOZ) of the Southern Ocean. J. Mar. Syst. (in press).

Ramonet, M. 1994. Variabilité du CO_2 atmosphérique en régions australes: comparaison modèle/mesure. Thèse d'Université Paris VII, 221 pp.

Redfield, A. C., B. H. Ketchum and F. A. Richards. 1963. The influence of organisms on the composition of sea-water, *in* The Sea, *2,* M. N. Hill, ed., Wiley-Interscience, NY, 26–77.

Robertson, J. E. and A. J. Watson. 1995. A summer-time sink for atmospheric carbon dioxide in the Southern Ocean between 88W and 80E. Deep-Sea Res., *42,* 1081–1091.

Sarmiento, J. L. and C. Le Quéré. 1996. Oceanic carbon dioxide uptake in a model of century-scale global warming. Science, *274,* 1346–1350.

Sarmiento, J. L., J. C. Orr and U. Siegenthaler. 1992. A perturbation simulation model of CO_2 uptake in an ocean general circulation model. J. Geophys. Res., *C97,* 3621–3645.

Siegenthaler, U. and J. L. Sarmiento. 1993. Atmospheric carbon dioxide and the ocean. Nature, *365,* 119–125.

Stoll, M. H. C., H. J. W. de Baar, M. Hoppema and E. Fahrbach. 1999. Early winter pCO_2 data revealing undersaturation in the fully ice covered Weddell Sea. Mar. Chem. (in press).

Takahashi, T., R. A. Feely, R. F. Weiss, R. H. Wanninkhof, D. W. Chipman, S. C. Sutherland and T. T. Takahashi. 1997. Global air-sea fluxes of CO_2: an estimate based on measurements of sea-air pCO_2 difference, *in* Revelle Symposium, Proc. Natl. Acad. Sci., C. D. Keeling, ed., *94,* Washington D. C., USA, 8292–8299.

Takahashi, T., J. Olafsson, J. G. Goddard, D. W. Chipman and S. C. Sutherland. 1993. Seasonal variation of CO_2 and nutrients in the high-latitude surface oceans: a comparative study. Global Biogeochem. Cycles, *7,* 843–878.

Tans, P. P., I. Y. Fung and T. Takahashi. 1990. Observational constraints on the global atmospheric CO_2 budget. Science, *247,* 1431–1438.

Taylor, A. H., A. J. Watson, M. Ainsworth, J. E. Robertson and D. R. Turner. 1991. A modelling investigation of the role of phytoplankton in the balance of carbon at the surface of the North Atlantic. Global Biogeochem. Cycles, *5,* 151–171.

Tréguer, P. and G. Jacques. 1992. Dynamics of nutrients and phytoplankton, and fluxes of carbon, nitrogen and silicon in the Antarctic Ocean. Polar Biol., *12,* 149–162.

Tréguer, P., D. M. Nelson, A. J. van Bennekom, D. J. DeMaster, A. Leynaert and B. Quéguiner. 1995. The silica balance in the world ocean: A reestimate. Science, *268,* 375–379.

Wanninkhof, R. H. 1992. Relationship between wind speed and gas exchange over the ocean. J. Geophys. Res., *C97,* 7373–7382.

Weiss, R. F. 1974. Carbon dioxide in water and seawater: The solubility of a non-ideal gas. Mar. Chem., *2,* 203–215.

White, W. B. and R. G. Peterson. 1996. An Antarctic circumpolar wave in surface pressure, wind, temperature and sea-ice extent. Nature, *380,* 699–702.

Winn, C. D., F. T. Mackenzie, C. J. Carrillo, C. L. Sabine and D. M. Karl. 1994. Air-sea carbon dioxide exchange in the North Pacific Subtropical gyres: implications for the global carbon budget. Global Biogeochem. Cycles, *8,* 157–163.

Received: 6 *January, 1998;* revised: *29 September, 1998.*